A CFD Study of the Performance of Horizontal Dilution Tubes

Hartmut Mätzing*, Petros Vlavakis, Dimosthenis Trimis** and Dieter Stapf***
contact: hartmut.maetzing@kit.edu
*Karlsruhe Institute of Technology (KIT), Institute for Technical Chemistry (ITC),
Hermann-von-Helmholtz-Platz 1, D-76344 Eggenstein-Leopoldshafen, Germany
**Karlsruhe Institute of Technology (KIT), Engler-Bunte-Institute (EBI-VBT),
Engler-Bunte-Ring 1, D-76131 Karlsruhe, Germany

Abstract
Since about 20 years, horizontal dilution tubes are in use to study soot formation close to the main reaction zone, in order to characterize the properties of nascent soot nanoparticles and to obtain insight into the soot formation process. In this study, the performance of horizontal dilution tubes, both free standing and embedded, is investigated by RANS and LES. The flame gas enters the dilution tube through a pinhole and, in experimental studies, it is claimed to mix quickly with the cold, inert gas flow in the dilution tube. Previously, the distortion of the flow and temperature profiles around the dilution tube were investigated. Here, the orifice flow as well as the dilution process inside the tube are studied. The volume flow through the orifice is shown to be proportional to the square root of the pressure drop. The discharge coefficient is the range 0.9 ± 0.3 in the cold air (calibration) case and drops to 0.35 under hot (flame) conditions. The resulting dilution ratio is roughly a factor of 5 below typical literature data. The gas sample is found to remain in the wall boundary layer and, the mixing process is not complete at the end of the dilution tube. Turbulence decays rapidly behind the tube inlet and, in the main body of the tube, the flow is in the laminar to turbulent transition regime. Turbulence increases significantly in the outlet section which has much smaller pipe cross sections. Despite its relatively low Reynolds number, the outlet flow to the particle sizer (or to the gas analyzer) is clearly turbulent and, interactions with the wall are probable. The results are in agreement with previous findings from laminar jets in crossflow. Guidelines for optimization of the sampling conditions are suggested.

Introduction
The combustion of fossil fuels, as well as that of CO_2 neutral alternatives, like biomass, in industrial firings can give rise to the formation of soot and other products of incomplete combustion. On the one hand, a certain amount of soot may be welcome, because it supports the heat transfer in industrial furnaces. On the other hand, soot as well as inorganic fly ash components stick to the boiler tubes, hence they need to be cleaned in regular intervals. Moreover, if emitted into the environment, in the form of submicron particles, soot is also viewed as hazard in terms of climate and health issues. It is therefore desirable to control and monitor soot formation in order to avoid expensive filters or other installations.
Soot formation in hydrocarbon flames has been studied for many years. It involves a gas to particle transition, heterogeneous particle growth and aerosol dynamics at high temperature. Early studies were performed with non-intrusive, optical techniques preferentially. Therefrom, it is known that the major part of the soot mass is formed by heterogeneous surface growth, while particle inception contributes only 10 - 20% to the total soot mass [1,2]. The precursors of the first, nascent soot particles were expected to be polycyclic aromatics (PAH) and finally, pyrene was included as key intermediate in soot formation in the so-called HACA mechanism (hydrogen abstraction, C_2H_2 addition) which is used to model soot formation numerically [3]. The modern research focuses on the experimental detection of further PAH-type precursors and on the feasibility to include them in soot formation models. In addition, it is discussed, how spherical structures can emerge from the interaction of planar precursors [4-6].
In this context, it is still interesting to study soot particle inception which in premixed flat flames occurs a little downstream of the main reaction zone where the particle number density can be around 10^{12} cm^{-3}, while the particle size is only a few nm. Under such conditions, non-intrusive optical measurements have limitations, because both light scattering and extinction are weak. Since about 20

years, an alternative particle counting and sizing method has become common. It involves the use of macroscopic (10 mm i.d.) horizontal dilution tubes for gas and particle sampling. Particle analysis is done by scanning mobility particle sizers (SMPS) which basically consist of a DMA (differential mobility analyser) for particle mobility and size analysis and of a CPC (condensation particle counter) for particle counting. The method was first proposed by Kasper et al. [7] and was further developed by Zhao et al. [8,9] who emphasized the need for high dilution ratios, because SMPS have an upper limit of particle number concentrations in the order of 10^6 - 10^7 cm^{-3}. The reliable particle sampling from a high temperature, reacting environment indeed requires a fast quenching and dilution process, in order to avoid further particle inception, surface growth and coagulation in the measurement device. Horizontal dilution tubes, fed with a cold, turbulent inert gas were expected to satisfy these requirements due to turbulent mixing of the small sample gas flow into the dilution gas flow. The sample gas flow enters the dilution tube through a small orifice (0.1 – 0.5 mm i.d.), driven by the pressure drop at the orifice. Since it is impractical to measure the sample gas flow directly under flame conditions, the orifice flow is usually measured under ambient air conditions and extrapolated to flame conditions. The extrapolation is usually performed with the assumption of Poiseuille flow in the orifice. As described in the Theory section below, a revised procedure based on Bernoulli's equation is proposed in this paper. In addition, it is emphasized here that the experimental setup corresponds to a jet in crossflow arrangement and the orifice flow can be understood and interpreted in terms of the corresponding flow characteristics. Finally, it has also become common to integrate the dilution tube into a cooled stagnation plate, so in addition to the CFD simulation of a free standing dilution tube, this case is considered also. While numerous studies have investigated the possible measurement errors associated to the introduction of macroscopic dilution tubes into the postflame gas [10-18], this paper considers the gas flow inside the dilution tube by Reynolds Averaged Navier Stokes (RANS) and Large Eddy Simulations (LES), in order to obtain better information about the mixing and quenching conditions and performance.

Theory

The orifice flow rate Q_{orf} is considered to be given by the isentropic flow rate according to Bernoulli's equation:

$$Q_{orf} = C_d \cdot A_{orf} \cdot \sqrt{2\,\Delta P_{orf} / \rho} \qquad (1)$$

Eq. (1) is valid for incompressible fluid flow (at Mach number < 0.3) and ρ is density, ΔP_{orf} is the pressure drop at the orifice, A_{orf} is the orifice cross section. C_d is the discharge coefficient, typically around 0.7 [19-21], but due to the presence of a crossflow, C_d may be larger than 1 [22].

The flame gas sampling can be understood to be a jet in crossflow arrangement, where the sample gas flow is the jet and the dilution gas flow is the crossflow. Jets in crossflow have a wide range of practical applications and have been investigated for many years [22-26]. Several characteristic numbers are used to describe their flow characteristics:

- the jet to crossflow velocity ratio $R = (\rho_j/\rho_\infty)^{0.5} \cdot v_j/v_\infty$
- the jet to crossflow density ratio $S = \rho_j/\rho_\infty$
- the jet to crossflow momentum flux ratio $J = R^2$
- the jet Reynolds number $Re_j = v_j D_j/\mu_j$, $\mu_j = \eta_j/\rho_j$

Therein, v is velocity, D is diameter, η is dynamic viscosity and μ is kinematic viscosity. Subscript j denotes the jet and ∞ denotes the crossflow. Experimentally, high R, J and Re_j were found to favour the mixing of the jet into the crossflow. At J < 5, the jet is known to adhere to the wall and not to mix well with the crossflow [24,25]. Such conditions are met under flame gas sampling conditions, where a high temperature, high viscosity jet enters into a much colder crossflow and, typical values are R = 0.14 – 0.77 and J = 0.02 – 0.6.

CFD Simulations

An uncooled, free standing ceramic (Al_2O_3) dilution tube with 9 mm i.d. and a pinhole of D_{orf} = 0.3 mm was used as base case [27]. The nitrogen dilution flow Q_{N2} was 30 slpm. In the experiment [27], the pressure drop between the measurement locations ΔP1 and ΔP2 in Fig. 1 was assumed to decrease linearly. The two outlets were in parallel at slightly different vertical positions. Another setup with outlets oriented perpendicularly was modelled earlier [28] with no difference in major findings. The calculations were performed for a single phase gas flow under cold (calibration) conditions and under hot (flame) conditions. The tube wall temperature was assumed to vary between 298 K and 1000 K under flame conditions as shown in Fig. 1, in agreement with literature reports [8,9,27]. The flame gas composition was taken to be x_{CO2} = 0.042, x_{CO} = 0.21, x_{H2} = 0.42, x_{H2O} = 0.268, x_{C2H2} = 0.03, x_{CH4} =

0.02 and x_{C2H4} = 0.01. It corresponds to an CH_4/O_2 oxy-fuel flame with equivalence ratio Φ = 2.4. The orifice volume flow was determined from the calculated mass flow rate and density. The dilution ratio is then given by DR = 1 + Q_{N2} [slpm]/Q_{orf} [slpm].

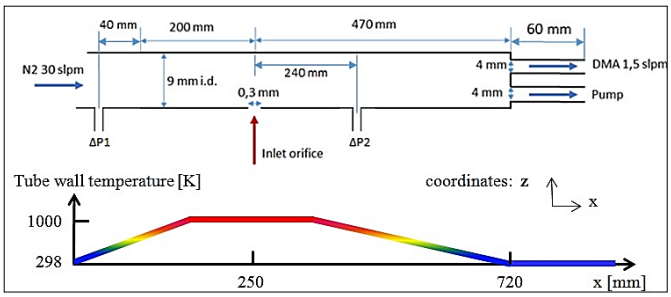

Figure 1. Geometry of the free standing dilution tube and wall boundary conditions.

Two meshes were generated with spatial resolutions of 170 μm and 30 μm. RANS calculations were performed with the SST k-ω turbulence model and near wall treatment was done by high resolution inflation layers. The same results were obtained with both meshes which confirms grid independence. The LES calculations were performed with the finer mesh using the Smagorinsky model for subgrid-scale modelling. Vortex detection was done using the Q criterion, the λ_2 criterion as well as pressure and velocity fluctuations [29].

Results

While the dilution gas flow enters the tube under turbulent conditions, it rapidly looses its turbulent properties and the Reynolds number decreases from 5000 at the inlet to 1500 at the location of the orifice (Fig. 2). Towards the DMA outlet, which carries only 5% of the total flow, it decreases further, while it increases significantly in the pump outlet. At the location of the orifice, the radial velocity profile indicates the flow to be in the laminar to turbulent transition regime [Fig. 3].

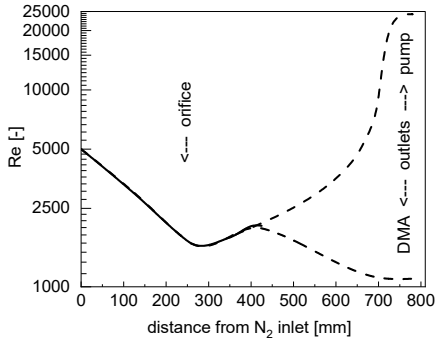

Figure 2. Sketch of the Reynolds number and flow splitting along the tube axis.

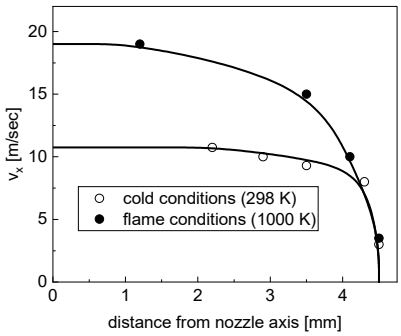

Figure 3. Radial velocity profile at the location of the orifice.

In agreement with this, only tiny and uniformly distributed vortex structures are detected in the main section of the dilution tube (Fig. 4) which indicates rather homogeneous flow conditions. In the outlet sections, large vortex structures are visible (Fig. 5), even in the DMA outlet despite its low Re number. Obviously, the length of the outlet tube is too small to level out the turbulent motion which originates from the region, where the flow splitting starts. This is illustrated further in Fig. 6 which compares the pathlines in the two outlets. While in the pump outlet, they are in parallel, they appear to be twisted or meandering in the DMA outlet. Turbulent flow at low Reynolds number is a wellknown phenomenon [30]. Moreover, in the results it is also seen that the sample gas flow does not mix well into the dilution gas flow. Rather, it remains in the relatively hot boundary layer at the tube wall and, consequently, concentration gradients develop in the middle section of the tube and persist in the outlet section (Fig. 7). Very similar results were obtained for embedded dilution tubes which differ from free standing tubes mainly by the much more intense cooling, down to roughly 400 K [18].

The calculated orifice flow rates for ambient air and for hot flame gas are shown in Fig. 8.a. The corresponding discharge coefficients are $C_{d,\,calc} = Q_{orf,\,calc} / Q_{orf,\,theoretical}$, where $Q_{orf,\,theoretical}$ is given by eq. (1) setting C_d = 1. For ambient air, C_d is close to 0.7 at low pressure drop, then it increases to a maximum of 1.25 at $\Delta P \approx 150$ Pa and it decreases towards higher pressure drop. This behaviour is in

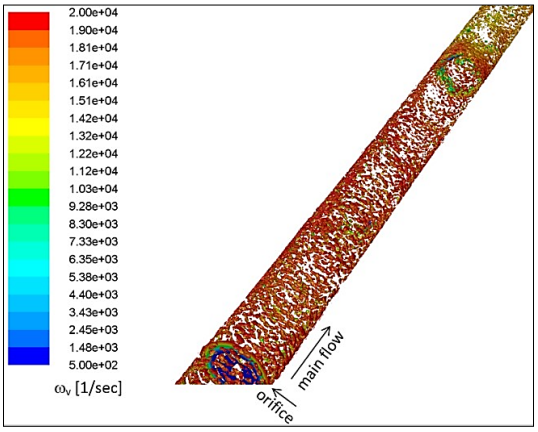

Figure 4. Iso-surface $\lambda_2 = -8 \cdot 10^4$ colored by vorticity from orifice location up to 200 mm downstream.

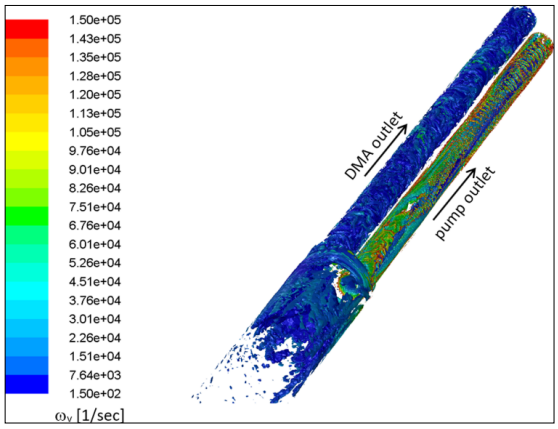

Figure 5. Iso-surface $\lambda_2 = -8 \cdot 10^4$ colored by vorticity in the outlet section.

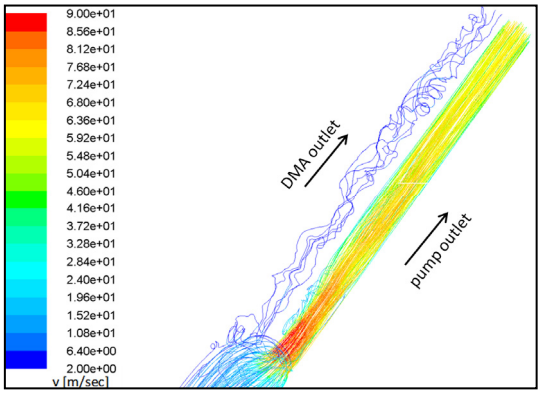

Figure 6. Trajectories in the outlets colored by velocity magnitude.

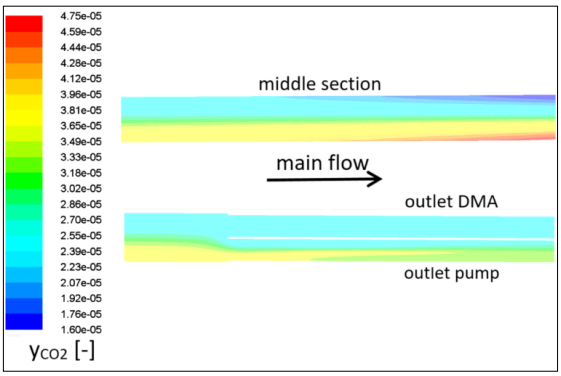

Figure 7. Mass fraction of CO_2 in the middle and in the outlet sections.

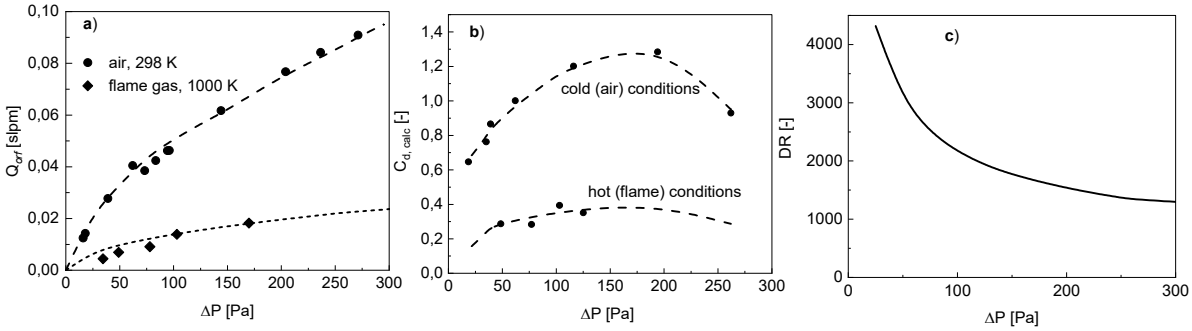

Figure 8. (a) Orifice flow, broken and dotted lines: eq. (1); (b) calculated discharge coefficients, broken lines: fit for cold (air) conditions and, fit using $C_d \propto \eta^{-1.75}$ for hot (flame) conditions; (c) calculated dilution ratio DR at the DMA outlet under flame conditions.

agreement with previous literature data [22]. Under flame gas conditions, C_d is much smaller and does not exceed 0.35. This is probably due to the increase of the gas viscosity at higher temperature and indeed, C_d appears to scale with $\eta^{-0.75}$ (Fig. 8.b). Fig. 8.c shows the calculated dilution ratio as function the pressure drop. The calculated DR is based on the area weighted average of the CO_2 mole fraction at the DMA outlet (see comment in the Discussion section).

Discussion

RANS calculations and LES were performed to study the gas flow and the mixing process in horizontal dilution tubes. It was found that the initial turbulence of the dilution gas flow rapidly decreases. Therefore, the flow is in the laminar to turbulent transition regime in the main part of the tube with Re

numbers ranging from 1500 - 2000. The turbulence increases again towards the outlet tubes which have a much smaller diameter than the dilution tube. In the pump outlet, Re numbers of $2 \cdot 10^4$ and higher are met. In the DMA outlet, which carries only about 5% of the total gas flow, Re decreases to roughly 1000, but vortex structures persist and the flow lines are seen to oscillate and to touch the outlet tube wall. This appears unfavorite for a reliable and reproducible gas and particle sampling.
Differently from previous reports, the orifice flow was described here by Bernoulli's equation and a discharge coefficient. Under low temperature (i.e. calibration) conditions, C_d was found to be in the range 0.6 – 1.25, with the maximum value reached at $\Delta P \approx 150$ Pa. Such a behaviour is in agreement with previous literature data [22]. Under hot (flame) conditions, C_d was found to be much smaller, below 0.4, which may be due to the higher gas viscosity at elevated temperature. Indeed, a correlation $C_d \propto \eta^{-1.75}$ appears to explain the results.
In a novel approach, the orifice flow was interpreted in terms of a jet in crossflow configuration. The the jet to crossflow momentum flux ratio was found to be extremely small which prevents efficient mixing according to previous literature reports. In fact, it is seen in the CFD results that the flame gas sample flow adheres to the wall or wall boundary layer and that concentration gradients persist along the cross section of the tube. It means that the mixing process remains incomplete at the available time scale. This is seen clearly in the results which show concentration gradients along the cross sections of the dilution tube and the tube outlets. Therefore, since dilution ratios are usually calculated with the assumption of complete, homogeneous mixing, they can only serve as rough estimates. In addition, experimental DRs have a tendency to turn out too high because of eventual clogging which decreases the orifice diameter. The uncertainties associated to clogging are approximately of the order of a factor 3 in dilution ratio [13]. The dilution ratios obtained in this study are about a factor of 5 below reported averages.

Conclusions

Horizontal dilution tubes are widely used in flame gas and soot particle sampling. The mixing and quenching processes in a horizontal dilution tube was investigated by RANS calculations and by LES. Two high resolution grids were used and grid independence of the results was confirmed.
The high initial turbulence intensity at the tube inlet was found to decline rapidly and, the dilution gas flow was found to be in the laminar to turbulent transition regime in the main part of the tube. Due to the temperature and viscosity difference of the gas flows, the mixing and cooling processes are slow. Therefore, the sample gas flow has a tendency to remain close to the tube wall and corresponding concentration gradients persist towards the end of the dilution tube, where the gas flow is split into comparatively small outlet pipes. Here, the turbulence intensity increases significantly and turbulent vortex structures develop which persist even in the outlet to the measurement device (DMA) despite the low Re number therein. Consequently, the flow lines appear to touch the outlet pipe wall many times which is disadvantageous for a reliable and reproducible sampling procedure. This behaviour was observed for the case of both free standing and embedded dilution tubes.
In a similar previous study [28], a different dilution tube configuration was investigated with pipe outlets perpendicular to each other. In addition, the tube diameter was a factor of two smaller and the tube material was steel instead of Al_2O_3. The major findings, however, were the same, hence it is concluded that the results truly reflect the flow properties for this type of jet in crossflow arrangements and are representative for most of the individual experimental setups.
In a situation of persisting concentration gradients, the concept of a dilution ratio with homogeneous mixing has a limited applicability. In this study, the DR was calculated using area weighted average concentrations at the DMA outlet and, the calculated values are a factor of 5 below typical reports in the literature.
To improve the performance of horizontal dilution tubes, it appears that the jet to crossflow momentum flux ratio should be increased. This may be achieved by applying a higher pressure drop at the orifice or by reducing the flow rate of the dilution gas. In addition, small obstacles might be installed in the dilution tube upstream of the orifice, in order to maintain a higher turbulence intensity. Also, a dilution gas of low viscosity/high diffusivity may improve the mixing process.

References

[1] Wagner, H.Gg., "Soot formation in combustion", *Symposium (International) on Combustion 17*, 1979, 3-19.
[2] Haynes, B.S., Wagner, H.Gg., "Soot formation", *Progress in Energy and Combustion Science 7*, 1981, 229-273.
[3] Appel, J., Bockhorn, H., Frenklach, M., "Kinetic modelling of soot formation with detailed chemistry and physics", *Combust. Flame 121*, 2000, 122-136.

[4] Wang, H., “Formation of nascent soot and other condensed-phase materials in flames”, *Proc. Combust. Inst. 33*, 2011, 41-67.
[5] Johansson, K.O., Head-Gordon, M.P., Schrader, P.E., Wilson, K.R., Michelsen, H.A., “Resonance-stabilized hydrocarbon-radical chain reactions may explain soot inception and growth”, *Science 361*, 2018, 997-1000.
[6] Frenklach, M., Mebel, A.M., “On the mechanism of soot nucleation”, *Phys. Chem. Chem. Phys. 22,* 2020, 5314-5331.
[7] Kasper, M., Siegmann, K., Sattler, K., “Evaluation of an in situ sampling probe for its accuracy in determining particle size distributions from flames”, *J. Aerosol Sci. 28*, 1997, 1569-1578.
[8] Zhao, B., Yang, Z., Johnston, M.V., Wang, H., Wexler, A.S., Balthasar, M., Kraft, M., “Measurement and numerical simulation of soot particle size distribution functions in a laminar premixed ethylene-oxygen-argon flame”, *Combust. Flame 133*, 2003, 173–188.
[9] Zhao, B., Yang, Z., Wang, J., Johnston, M.V., Wang, H., “Analysis of soot nanoparticles in a laminar premixed ethylene flame by scanning mobility particle sizer”, *Aerosol Sci. Technol. 37,* 2003, 611-620.
[10] Hansen, N., Cool, T.A., Westmoreland, P.R., Kohse-Höinghaus, K., “Recent contributions of flame-sampling molecular-beam mass spectrometry to a fundamental understanding of combustion chemistry”, *Prog. Energy Combust. Sci. 35,* 2009, 168-191.
[11] Skovorodko, P., Tereshchenko, A., Korobeinichev, O., Knyazkov, D., Shmakov, A.G., “Experimental and numerical study of probe-induced perturbations of the flame structure”, *Combust. Theor. Model. 17,* 2013, 1-24.
[12] Egolfopoulos, F.N., Hansen, N., Ju, Y., Kohse-Höinghaus, K., Law, C., Qi, F., “Advances and challenges in laminar flame experiments and implications for combustion chemistry”, *Prog. Energy Combust. Sci. 43,* 2014, 36-67.
[13] Abid, A.D., Heinz, N., Tolmachoff, E.D., Phares, D.J., Campbell, C.S., Wang, H., “On evolution of particle size distribution functions of incipient soot in premixed ethylene–oxygen–argon flames”, *Combust. Flame 154,* 2008, 775-788.
[14] Camacho, J., Liu, C., Gu, C., Lin, H., Huang, Z., Tang, Q., You, X., Saggese, C., Li, Y., Jung, H., Deng, L., Wlokas, I., Wang, H., “Mobility size and mass of nascent soot particles in a benchmark premixed ethylene flame”, *Combust. Flame 162,* 2015, 3810-3822.
[15] Commodo, M., De Falco, G., Bruno, A., Borriello, C., Minutolo, P., D’Anna, A., “Physicochemical evolution of nascent soot particles in a laminar premixed flame: from nucleation to early growth”, *Combust. Flame 162,* 2015, 3854-3863.
[16] Ghiassi, H., Jaramillo, I.C., Toth, P., Lighty, J.S., “Soot oxidation-induced fragmentation: Part 2: Experimental investigation of the mechanism of fragmentation”, *Combust. Flame 163,* 2016, 170-178.
[17] Tang, Q., Mei, J., You, X., “Effects of CO_2 addition on the evolution of particle size distribution functions in premixed ethylene flame”, *Combust. Flame 165,* 2016, 424-432.
[18] Saggese, C., Cuoci, A., Frassoldati, A., Ferrario, S., Camacho, J., Wang, H., Faravelli, T., “Probe effects in soot sampling from a burner-stabilized stagnation flame”, *Combust. Flame 167*, 2016, 184-197.
[19] Lafferty, J.M. (Ed.), *Foundations of vacuum science and technology*, Wiley, N.Y., 1998.
[20] Borutzky, W., Barnard, B., Thoma, J., “An orifice flow model for laminar and turbulent Conditions”, *Simul. Modelling Practice Theory 10*, 2002, 141-152.
[21] Oertel, H., Prandtl, L., Böhle, M., *Prandtl – Führer durch die Strömungslehre*, Vieweg + Teubner, Wiesbaden, 2008.
[22] Berger, S., Gourdain, N., Bauerheim, M., Devillez, S., “Discharge coefficient of an orifice jet in crossflow: influence of inlet conditions and optimum velocity ratio”, AIAA Aviation 2019 Forum, Dallas, US, June 2019, https://hal.archives-ouvertes.fr/hal-02166754.
[23] Muppidi, S., Mahesh, K., “Study of trajectories of jets in crossflow using direct numerical simulations”, *J. Fluid Mech. 530*, 2005, 81-100.
[24] Mahesh, K., “The interactions of jets with crossflow”, *Annu. Rev. Fluid Mech. 45*, 2013, 379-407.
[25] Karagozian, A.R., “The jet in crossflow”, *Phys. Fluids 26*, 2014, 101303.
[26] Chang, J., Shao, X., Hu, X., Zhang, S., “Flow characteristics of a low Reynolds number jet in crossflow with an obstacle block”, *The Open Fuels & Energy Science Journal 9*, 2016, 1876-973X/16.
[27] Frenzel, I., Krause, H., Trimis, D., “Study on the influence of ethanol and butanol addition on soot formation in iso-octane flames”, *Energy Procedia 120*, 2017, 721-728.
[28] Mätzing, H., Stapf, D., “Modelling soot particle inception and soot particle probe sampling”,

ECM 2019 - 9th European Combustion Meeting, Lisbon, Apr. 14-17, paper S1_R1_78, https://doi.org/10.5445/IR/1000094019.
[29] Holmen, V., *Methods for vortex identification*, MA Thesis, Lund University, 2012, https://lup.lub.lu.se/student-papers/search/publication/3241710.
[30] Tsukahara, T., Seki, Y., Kawamura, H., Tochio, D., “DNS of turbulent channel flow at very low Reynolds numbers”, *4th Int. Symp. on Turbulence and Shear Flow Phenomena*, Williamsburg, VA, USA, 27-29 Jun. 2005, pp. 935-940.